ISBN: 978-3-95450-262-2 ISSN: 2673-5350 doi: 10.18429/JACoW-IBIC2025-WEPMO34

LONGITUDINAL BUNCH PROFILE RECONSTRUCTION VIA CHERENKOV RADIATION IN OPTICAL FIBERS

P. Pushkarna*, P. J. Giansiracusa[1], R. P. Rassool, S. L. Sheehy[2], G. N. Taylor, J. Valerian, M. Volpi
University of Melbourne, Melbourne, Australia
P. Bennetto, R. Dowd, Y-R. E. Tan
Australian Synchrotron - ANSTO, Clayton, Australia
[1]Also at Australian Synchrotron - ANSTO, Clayton, Australia
[2]Also at ANSTO, Lucas Heights, Australia

Abstract

Optical beam diagnostics, such as OTR (Optical Transition Radiation) screens and streak cameras, can overcome bandwidth limitations of electronic diagnostics. However, efficient light collection and transport is challenging. At the PEER (Pulsed Energetic Electrons for Research) facility at the AS (Australian Synchrotron), we use Cherenkov radiation (ChR) generated in optical fibers to reconstruct longitudinal bunch profiles at ps timescales, using a streak camera. This is enabled by proportionality of emitted ChR intensity to incident charge, when electrons directly impact the fiber. Streak cameras have been used to image ChR, but generating and transporting ChR in the same fiber is novel, and simplifies diagnostic design. We present bunch profile measurements using this technique, and assess its feasibility. We quantify distortion of ChR due to modal and chromatic dispersion in the fiber, survey methods to reduce distortion, and improve signal-to-noise ratio. Bunch profile measurements at ps resolution could allow bunch purity optimisation and detection of microbunching, previously not possible at PEER. This will greatly benefit PEER users, as well as beam quality in the booster and storage rings of the AS.

LONGITUDINAL DIAGNOSTICS AT PEER

The PEER (Pulsed Energetic Electrons for Research) beamline at the AS (Australian Synchrotron) is a 100 MeV linear electron accelerator, providing electron beams for radiotherapy and dosimetry studies [1, 2], particle and detector physics [3], and fundamental accelerator science [4]. PEER seeks a sub-ns longitudinal bunch profile diagnostic to improve bunch purity. This is challenging with existing diagnostics, since Fast Current Transformers, (FCTs) and Wall Current Monitors, (WCMs) with 1 GHz bandwidth are not able to resolve previously simulated 3 GHz satellite bunches imposed upon the main 500 MHz RF bucket by S-band accelerating structures [5]. The distribution of S-band microbunches within the main RF bucket has not yet been measured.

This contribution details a picosecond longitudinal bunch profile diagnostic developed for PEER by exploiting the Cherenkov effect in optical fibers. It details direct irradiation of multimode optical fibers with 100 MeV electron bunches to produce Cherenkov radiation (ChR), which is propagated in the same fibers toward a streak camera for detection at few-picosecond resolution. Bunch profiles are reconstructed by visualising ChR intensity with time, and the impacts of pulse broadening in the fiber due to modal and chromatic dispersion are considered.

Existing tunnel layout and engineering constraints at PEER hinder retrofitting in-air optical transport lines for OTR (Optical Transition Radiation) or ChR. Direct bunch streaking with a deflecting cavity is unfeasible due to the lack of additional RF power. Involved in-vacuum optical setups and demanding laser requirements disqualified EO techniques (Electro-Optical techniques). While bandwidths of available in-flange FCTs and Faraday Cups increase, an upgradeable photodetector located outside the accelerator tunnel was desired, to enable future bandwidth increases without disturbance to vacuum and beamline components.

Inspired by ChR fiber beam loss monitors [6, 7], optical fibers are considered a flexible solution to transport light outside the accelerator tunnel from previously inaccessible locations, and this has been demonstrated previously with Synchrotron Radiation (SR) [8]. Several works detail longitudinal phase space measurements using ChR generated in thin dielectric radiators [9], or non-invasively via Cherenkov diffraction radiation (ChDR) [10, 11]. This contribution is novel in combining generation and transport of ChR, simplifying and improving light coupling and easing transport.

DETECTOR CONFIGURATION

A brief overview of PEER is presented in Fig. 1. A dc 90 kV thermionic gun accelerates electrons toward the Subharmonic pre-buncher (SPB), a 50 mm 500 MHz standing-wave RF cavity operated in $\pi/2$ mode. Bunches are then captured by the Primary Bunching Unit (PBU), with four 3 GHz 20 mm cells, and accelerated from 90 keV to roughly 300 keV. The 3 GHz Final Bunching Unit (FBU), consisting of 16 42.22 mm cells, β-matches bunches with two travelling wave 3 GHz S-band accelerating structures, which increase energy to the nominal 100 MeV [12]. The linac is operated in "single-bunch" mode, which means that one 500 MHz RF bucket is filled, but may contain more complex 3 GHz microstructure whose observation is desired.

At the PEER in-air endstation, electron bunches directly impinge 15 m 105 µm 0.10 NA multimode silica optical fiber, angled at 47 degrees (the ChR emission angle in silica) to the beam with a Zaber X-RSW-E remotely controlled ro-

* pushkarnap@student.unimelb.edu.au

ISBN: 978-3-95450-262-2 ISSN: 2673-5350 doi: 10.18429/JACoW-IBIC2025-WEPMO34

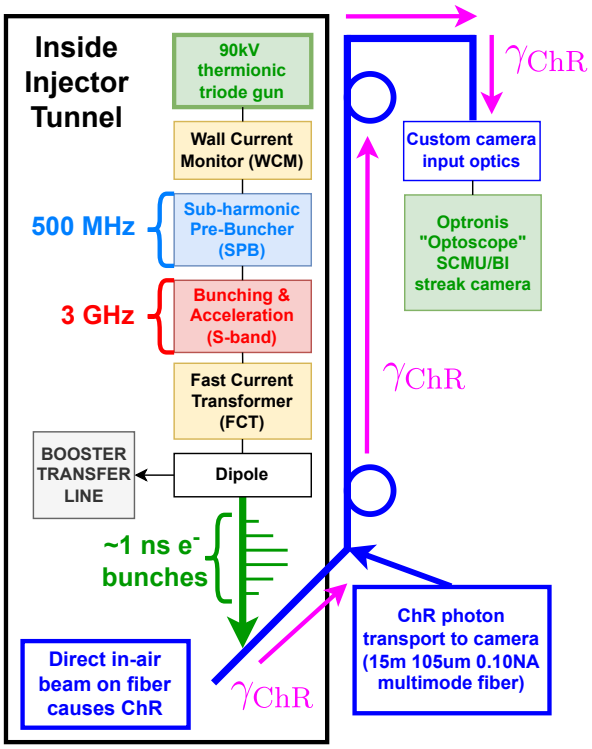

Figure 1: Block schematic of PEER beamline, in-air end-station and fiber configuration. Focussing solenoids and quadrupoles omitted for clarity.

tation stage. Aligning the fiber at the ChR angle in silica has been demonstrated to increase ChR light intensity at least three-fold, as more ChR rays are launched parallel to the fiber meridian, improving capture likelihood [13]. As streak cameras demands higher light intensity than more photosensitive detectors like photomultiplier tubes or silicon photomultipliers, optimising light intensity is crucial for maximising signal to noise ratio.

The fiber propagates ChR to an Optronis "Optoscope" SCMU-ST/BI streak camera, which is operated in synchroscan mode using the 500 MHz master oscillator (same as the SPB) and CCD camera acquisition is triggered with the same TTL (Transistor-Transistor Logic) pulse as that for the dc gun trigger. While capable of dual sweep axes, the streak camera is operated in single sweep mode with streaking plates calibrated at 50ps/mm, since ChR light intensity was still not sufficient to support detection with dual sweeping enabled. Streak images presented here thus have one axis static, with variations in light intensity corresponding to a spatial coordinate on the streak camera cathode, rather than time coordinate. In synchroscan mode, the oscillation of the master RF signal is used as the sweeping voltage, and the master RF phase can be changed locally at the streak camera to sample different sections of the incident light pulse. The RF phase is indicated in percentages of a full master RF synchroscan period throughout this proceeding.

Finally, the existing streak camera input optics (slit, micrometer, and compound Nikon AF-NIKKOR 35mm f/2 lens [14]) was replaced with single bi-convex focussing lens and adjustable tube-mounted bellows so that spot size on the camera cathode could be changed. A manual shutter was incorporated to prevent cathode overexposure. This was undertaken to further reduce light loss due to the large compound lens.

STREAK CAMERA RESPONSE

The PIL067-FS $O(25\,\text{ps})$ pulsed laser was triggered simultaneously with the streak CCD to test customised input optics and response of the streak camera to a known pulse profile. Figure 2 shows the response to 100 pulses acquired, with peaks centred and overlayed on the same time axis in black. The laser pulse tail does not decay smoothly to zero, rather the laser continues to emit light for some 100 ps after the main peak, which explains the larger trailing signals seen in Fig. 2. The Full-Width-At-Half-Maximum (FWHM) pulse width recorded was 24.33±4.04 ps, within expected laser specifications. This indicates that the resolution required to resolve 3 GHz substructures within a single RF bucket, could be reached.

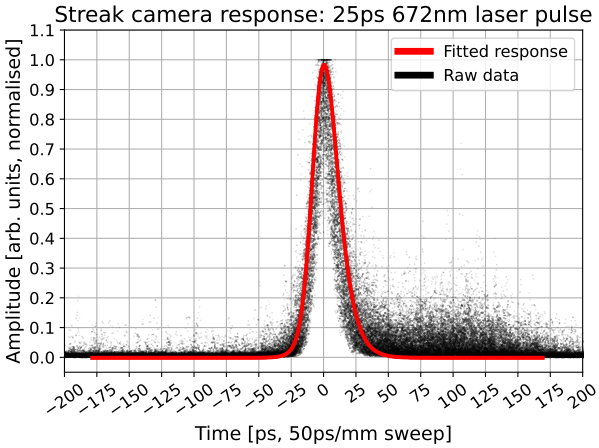

Figure 2: Response of streak camera to 25-30ps 672nm laser pulse, with the average of Skew-Gaussian pulses fitted to each streak frame projection shown in red.

Figure 3 shows the ChR fiber light pulse as recorded at the streak camera from direct beam irradiation of the fiber, and after travelling 15 m along the fiber cable length. Each panel (left to right) indicates an average of 20 streak images accumulated at a single value of the synchroscan phase, indicated in the subtitle of each panel. 20 images were averaged for each phase position as light intensity in single shot still presented poor signal-to-noise ratios. This makes further analysis prey to blurring from jitter in the master RF synchroscan signal, which is the sweep voltage for the 50 ps/mm plates.

To estimate jitter, the centre-of-mass (COM) position of single images along the time axis was determined. Over a set

ISBN: 978-3-95450-262-2 ISSN: 2673-5350 doi: 10.18429/JACoW-IBIC2025-WEPMO34

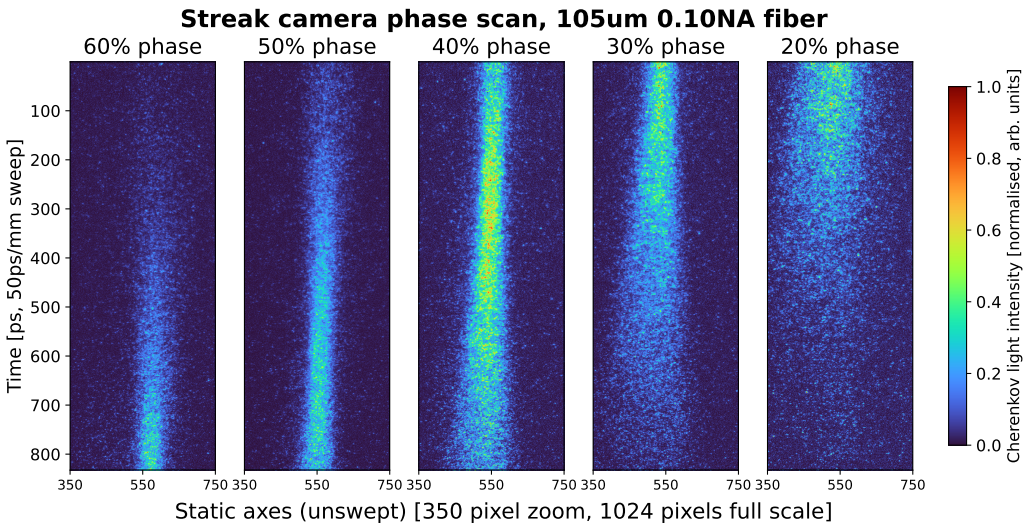

Figure 3: Streak camera signal for ChR emitted in multimode fiber. Notably, the horizontal axis records the "fanning out" of ChR as modes arriving later are more dispersed, and have a greater exit angle with respect to the fiber endface.

of 100 images taken from 5 different values of synchroscan phase the FWHM jitter (displacement from mean COM) was 37.6±2.2 ps. While signal features on $O(100\,\text{ps})$ timescales may be discernible, finer details may be distorted due to jitter and the image averaging process.

A notable feature in Fig. 3 is the spreading out of ChR as latter parts of the light pulse are sampled in the phase scan. Assuming a ray model for ChR modes launched in the fiber, modes propagating collinearly or with a shallow angle to the fiber meridian (central-axis) will travel a path length shorter than that of modes reflecting from the core cladding boundary several times. Qualitatively, these meridional modes should exit the fiber earlier, and at shallower angles as compared to skew modes. The static axis evidences this geometric effect, as ChR arriving in later panels (phase 20 %, 30 %) is more dispersed along the static (spatial) axis than ChR arriving from the bulk of the electron bunch (phase 40 %) or from the start (phase 60 %). Combined, we estimate the rms broadening due to modal dispersion from 15 m 0.10 NA fiber and synchroscan jitter, added in quadrature to be approximately 150 ps [15].

Fanning out of ChR along the static axis permits spatial filtering during post-processing to select the modes undergoing least dispersion. As more dispersed modes arrive later, a definite orientation of the time axis can also be deduced independently of the synchroscan sweep direction. This expedites stitching of images acquired from different positions in the phase scan to reconstruct the final bunch profile. Stitching was undertaken by manually matching the amplitudes and positions of spatially filtered projections from successive phase points, with the results indicated in Fig. 4, after applying a quadratic Savitzky-Golay low-pass smoothing filter, 100 samples wide. Figure 4 reveals that despite large rms broadening, modulations and asymmetry within the 1 ns are discernible, but do not yet correspond directly to the 3 GHz microbunching or a subharmonic thereof.

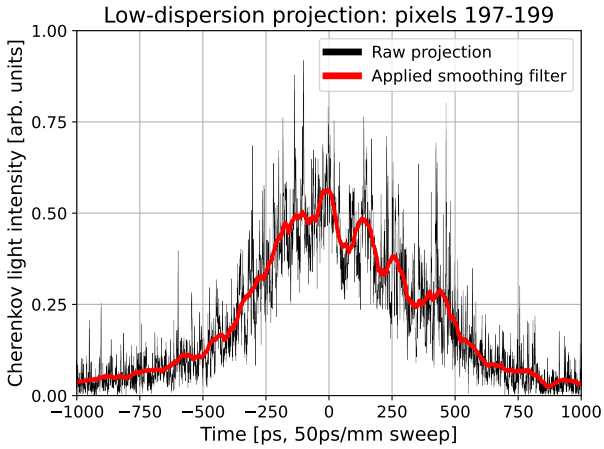

Figure 4: Stitched and spatially filtered projection, as deduced from Fig. 3.

CONCLUSION

This proceeding demonstrates the feasibility of generating and transporting ChR in optical fibers to undertake longitudinal phase space diagnostics at picosecond resolution. Streak camera optics will be further optimised to increase light yield, making single shot measurements feasible. Streak camera data will be compared by measurements of ChR with a Hamamatsu G4176 30 ps rise time photodiode, and correspondence with presented results verified. Optical fiber diagnostics represent a flexible and cost-effective means for monitoring of future accelerators, and can be conveniently retrofitted to existing machines.

ACKNOWLEDGEMENTS

The authors would like to gratefully acknowledge The Australian Synchtrotron Physics and Operations team for making this work possible.

ISBN: 978-3-95450-262-2 ISSN: 2673-5350 doi: 10.18429/JACoW-IBIC2025-WEPMO34

REFERENCES

[1] J. Cayley *et al.*, "Moskin dosimetry for an ultra-high dose-rate, very high-energy electron irradiation environment at peer", *Front. Phys.*, vol. 12, 2024. doi:10.3389/fphy.2024.1401834

[2] J. Valerian, P. Giansiracusa, M. Volpi, P. Pushkarna, R. Rassool, and S. Sheehy, "Optimising focusing parameters of very high energy electron beams for radiotherapy using Monte Carlo simulation", in *Proc. IPAC'25*, Taipei, Taiwan, Jun. 2025, paper TUPB042, to be published.

[3] S. Dekkers, "Searching for muon to electron conversion with the comet experiment", *Phys. Sci. Forum*, vol. 8, no. 1, 2023. doi:10.3390/psf2023008004

[4] P. Pushkarna *et al.*, "Searches for RF breakdown precursors using Cherenkov light in optical fibers", in *Proc. IPAC'25*, Taipei, Taiwan, Jun. 2025, paper MOCN3, to be published.

[5] C. Christou, V. Kempson, K. Dunkel, and C. Piel, "The pre-injector linac for the diamond light source", paper MOP21, pp. 84–86, 2004.

[6] P. J. Giansiracusa, "An Optical Fibre Beam-Loss Monitor for the Australian Synchrotron", Ph.D. thesis, University of Melbourne, Melbourne, Australia, Feb. 2021.

[7] M. Kastriotou, "Optimisation of Storage Rings and RF Accelerators via advanced Optical Fibre-based Detectors", Ph.D. thesis, University of Liverpool, Liverpool, UK, May 2018.

[8] M.-D. Noll *et al.*, "Towards fiber optics-guided synchrotron radiation-based longitudinal beam diagnostics at the KARA booster synchrotron", in *86th Jahrestagung der DPG und DPG-Frühjahrstagung der Sektion Materie und Kosmos-Arbeitskreis Beschleunigerphysik (SMuK 2023)*, Dresden, Germany, Mar. 2023.

[9] K.-i. Nanbu *et al.*, "Bunch length measurement employing Cherenkov radiation from a thin silica aerogel", *Particles*, vol. 1, no. 1, pp. 305–314, 2018. doi:10.3390/particles1010025

[10] A. Curcio *et al.*, "Noninvasive bunch length measurements exploiting Cherenkov diffraction radiation", *Phys. Rev. Accel. Beams*, vol. 23, no. 2, p. 022 802, 2020. doi:10.1103/PhysRevAccelBeams.23.022802

[11] C. Davut *et al.*, "Design and experimental verification of a bunch length monitor based on coherent Cherenkov diffraction radiation", *Phys. Rev. Res.*, vol. 7, no. 1, p. 013 193, 2025. doi:10.1103/PhysRevResearch.7.013193

[12] E. Meier, R. Dowd, and G. LeBlanc, "Characterization of the Australian synchrotron linac", *Nucl. Instrum. Methods Phys. Res. A*, vol. 589, no. 2, pp. 157–166, 2008. doi:10.1016/j.nima.2008.02.009

[13] S. Benítez, B. Salvachúa, and M. Chen, "Beam loss detection based on generation of Cherenkov light in optical fibers in the CERN Linear Electron Accelerator for Research", *Phys. Rev. Accel. Beams*, vol. 27, no. 5, p. 052 901, 2024. doi:10.1103/PhysRevAccelBeams.27.052901

[14] K. Rockwell, Nikon 35mm f/2 AF and AF-D NIKKOR (1989-), Jul. 2012. https://www.kenrockwell.com/nikon/35af.htm

[15] F. Mitschke, *Fiber optics*. Springer Berlin, 2016. doi:10.1007/978-3-662-52764-1